

The Implementation of Mixing Vane Directed Cross Flow Model in CUPID for Subchannel Scale T/H Analysis

Seul-Been Kim^a, Jae-Ho Lee^a, Goon-Cherl Park^a, Hyoung-Kyu Cho^{a*}

Department of Nuclear Engineering, Seoul National University, 1 Gwanak-ro, Gwanak-gu, Seoul 08826

Corresponding author: chohk@snu.ac.kr

1. Introduction

Recently, the necessity of high-fidelity and multi-physics simulation is increased. To achieve improved margin management, it is required that the PWR whole core analysis with coupled T/H (Thermal-Hydraulics) and neutronics code. For the pin-by-pin coupled calculation, the subchannel scale analysis could be an applicable tool as a T/H simulation tool. The higher accuracy of subchannel scale T/H analysis could be guaranteed than assembly scale analysis. Also, subchannel scale analysis provides endurable calculation time than CFD scale analysis.

CUPID is a multi-dimensional two-phase flow analysis code developed by KAERI for the component scale analysis of nuclear reactor. In recent times, the capability of CUPID was expanded on the subchannel scale T/H analysis. Some fundamental subchannel models like axial friction model, lateral form loss model, turbulent mixing and void drift model were implemented. Those models were validated against various subchannel experiments.

In the present study, the mixing vane model was implemented for the considering additional coolant transfer due to the structure of mixing vane. Afterwards, the DNBR analysis was conducted for investigating the effects of mixing vane on the DNBR distribution. For the verification, the single assembly of APR1400 was simulated with non-uniform power density distribution.

2. Implementation of Mixing Vane Directed Cross Flow Model to CUPID

The high temperature and pressure of the PWR core could induce the bending or vibration of the fuel rod. These lateral deformations of fuel rods are possible to damage the integrity of rod bundle due to the blockage of subchannel or the reduced cooling ability of coolant. For this reason, the spacer grid should provide lateral supporting force to the rod bundle to maintain the shape of fuel assembly.

There are several types of spacer grid depending on its purpose. For example, APR1400 uses various kinds of spacer grid to support the fuel rod, likes top-and-bottom grid, protective Inconel grid and mid-grids with mixing vanes. Top-and-bottom and protective Inconel grid hold the fuel rod to prevent the lateral movement and disturb the axial trembling by the friction between spacer grid and fuel bundle. Furthermore, mid-grids with mixing vane additionally induce the mixing of coolant within the assembly. This transfer of coolant

between adjacent subchannels could change the coolant and cladding surface temperature distribution and minimum DNBR. Hence, it is necessary to implement not only spacer grid model but also mixing vane model for more accurate subchannel scale T/H analysis.

Mixing vanes generate coolant transfer between adjacent channels. The direction of fluid is decided by configuration of mixing vane blade. The simplified coolant direction which is parallel with normal vector of the subchannel is presented in Fig. 1. To simulate this transference, the grid-directed cross flow model used in CTF [1] was implemented in CUPID [2].

In the case of CTF, the grid directed cross flow model is added on the momentum conservation equation solely. Since CUPID uses cell-centered collocated grid while CTF uses a staggered grid, the direct implementation of the CTF model on CUPID could cancel the momentum in inwards direction and decrease the effect of the mixing caused by the mixing vane. As a result, the exchange of mass and energy can be under-estimated in a code using the collocated grid scheme. Therefore, an additional scalar transfer between adjacent subchannels should be modeled. For the simulation, the mixing vane model was implemented on liquid mass, momentum and energy conservation equation of CUPID as follows:

$$\begin{aligned} M_e &= fu_l \rho_l A \\ M_k &= f^2 u_l \rho_l A \times u_l \\ M_h &= fu_l \rho_l A \times h_l \end{aligned} \quad (1)$$

where M_e, M_k, M_h : mass, momentum and energy transfer due to mixing vane model
 f : Lateral convection coefficient
 u_l : Axial liquid velocity
 A : Flow area

2.1.1. Model application on single assembly

For the preliminary simulation of the APR1400 single assembly with the mixing vane model, the direction of coolant between subchannels was decided from the shape of the blade on mixing vane. The distribution of lateral coolant transfer induced by mixing vane is described on the Fig. 2 (a). Fig. 2 (b) shows the flow pattern near the guide tubes in the corner and the center of the assembly, respectively. Among the five guide tubes in a single assembly, the

coolant passes through the four corner guide tubes as shown in left side of Fig. 2 whereas it is slightly blocked by the guide tube illustrated by right side of Fig. 2.

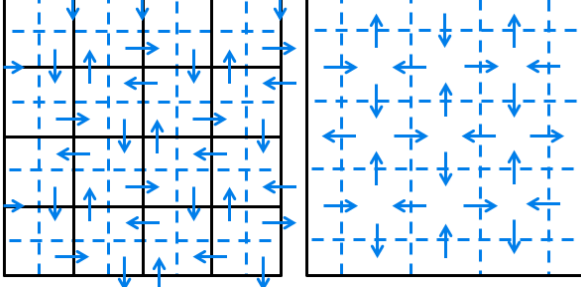
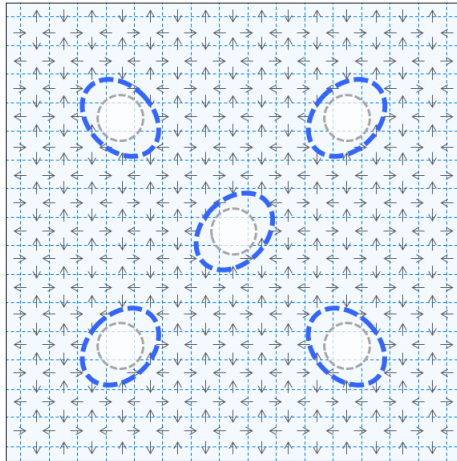
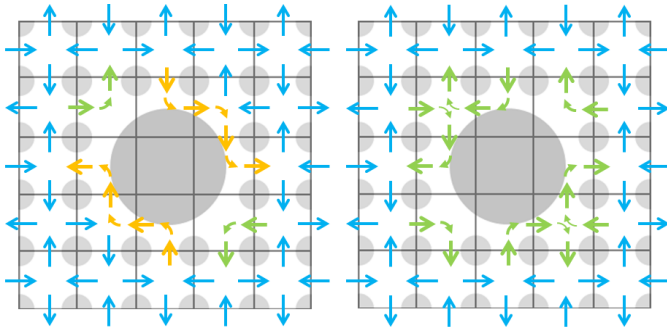


Fig. 1. The simplified mixing vane for subchannel scale analysis



(a) Schematic view of lateral coolant transfer induced by mixing vane in single assembly



(b) The lateral coolant transfer near the guide tubes in the corner of assembly (left) and center of assembly (right)

Fig. 2. The lateral coolant transfer direction induced by mixing vane

For the identification of DNBR distribution influenced by mixing vane model, a CHF correlation was implemented on CUPID. Since the KCE-1 CHF correlation which has been used for thermal margin calculation of APR1400 core is not open published, CE-1 CHF correlation [3] was implemented on CUPID for

preliminary simulation. The detail of CE-1 CHF correlation as follows:

$$q_{crit}'' = \frac{A'(A - BX)}{C} \times 10^6 \text{ Btu} / \text{hr} \text{ ft}^2 \quad (2)$$

$$\text{where } A' = b_1 \left(\frac{d}{d_m} \right)^{b_2}, A = (b_3 + b_4 p) G^{(b_5 + b_6 p)}$$

$$B = GH_{fg}, C = G^{(b_7 p + b_8 G)}$$

$b_1 \sim b_8$: Coefficient

G : Mass flux $\times 10^6 \text{ lb} / \text{hr} \text{ ft}^2$

p : Pressure, psia

X : Quality

H_{fg} : Latent heat of evaporation

d : Subchannel equivalent diameter, in

d_m : Matrix channel equivalent diameter, in

Table I: Parameters for CE-1 CHF correlation

b_1	2.8922×10^{-3}	b_2	-0.50749
b_3	405.32	b_4	-9.9290×10^{-2}
b_5	-0.67757	b_6	6.8235×10^{-4}
b_7	3.1240×10^{-4}	b_8	-8.3245×10^{-2}

3. Verification of The Mixing Vane Model using Non-uniform Power Density Distribution

The simulation of APR1400 single assembly using mixing vane model was progressed. The change of coolant and cladding surface temperature distribution and minimum DNBR were observed. The power distribution of individual rod was from the calculation result of neutronics code, nTRACER [4].

The power distribution of single assembly which has highest power density (assembly 23) and relatively lower power density (assembly 24) were used to reproduce the APR1400 power distribution on CUPID. The Fig. 3 describes the locations of each assembly.

As illustrated by Fig. 4, the local maximum power density of assembly 23 and assembly 24 are in the corner subchannel and the center subchannel. The location of maximum axial power density ratio is 2.22 m in both assemblies.

In the previous study [5], the lateral convection coefficient for mixing vane grid used for PSBT experiment [6] was determined as 0.27. This lateral convection coefficient f was adapted for this simulation.

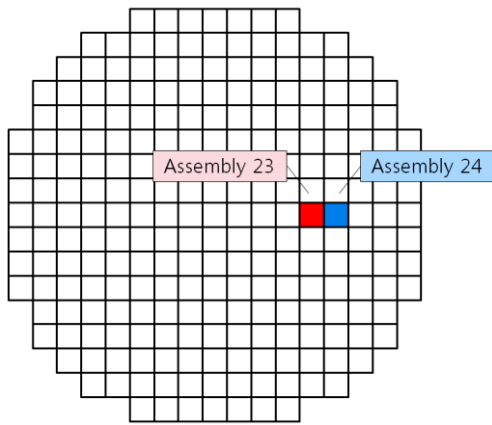


Fig. 3. Location of the imposed power distribution of the calculation of single assembly

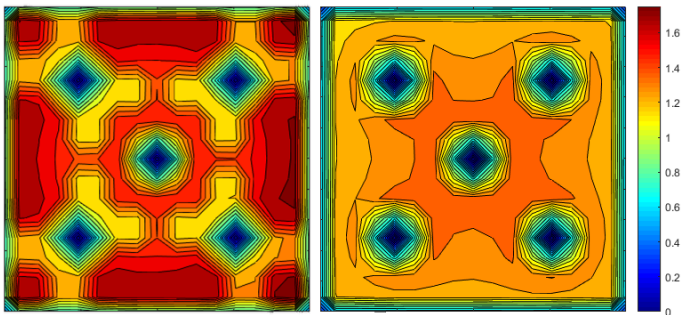


Fig. 4. Power density ratio of assembly 23 (left) and assembly 24 (right) at the 2.22m

3.1. Assembly with corner-maximum power density (assembly 23)

The lateral velocity distribution induced by mixing vane model is shown as Fig. 5. The relatively strong rotation of coolant near the guide tube could be observed. This momentum transfer between subchannels near the guide tube diminishes the temperature gradient. Due to the effect of the guide tube, the gradient of coolant and cladding surface temperature are reduced as described in Fig. 6 and Fig. 7. Without mixing vane model, the maximum coolant and cladding surface temperature at the outlet were 607.969 K and 608.825 K at the corner. After the implementation of mixing vane model, the maximum temperatures were reduced to 606.251 K and 607.068 K.

The lateral and axial location of minimum DNBR was maintained as corner cell and 1.98 m. The minimum DNBR is increased by 1.429 % with the mixing vane model. The calculated DNBR distribution is presented on Fig. 8.

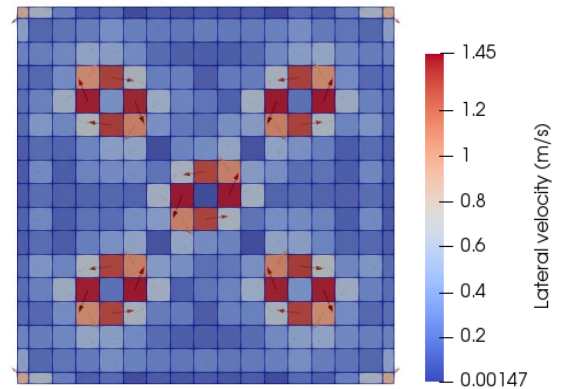


Fig. 5. Lateral velocity distribution with mixing vane model

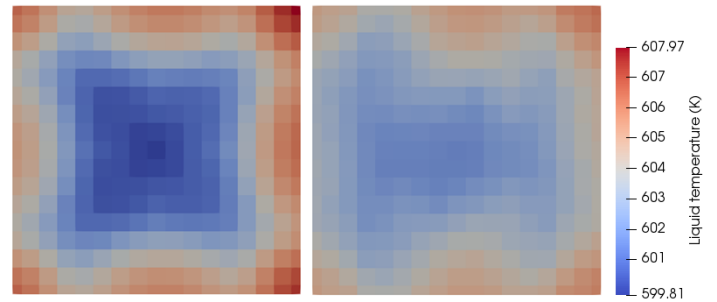


Fig. 6. Outlet coolant temperature distribution without mixing vane model (left) and with mixing vane model (right)

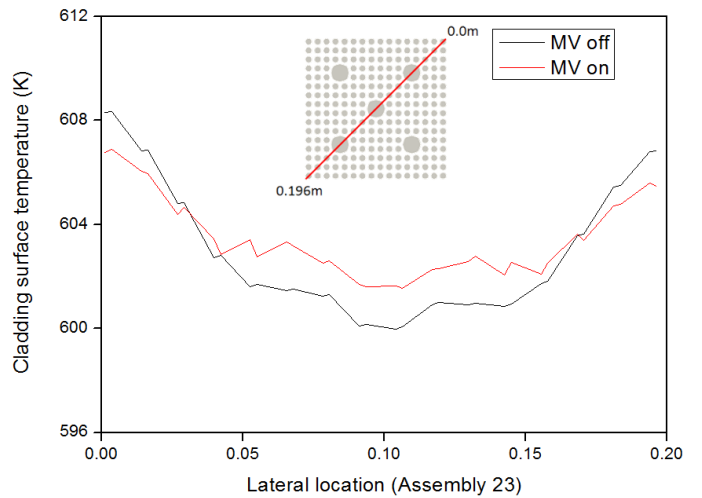


Fig. 7. Outlet cladding surface temperature distribution using power density of assembly 23

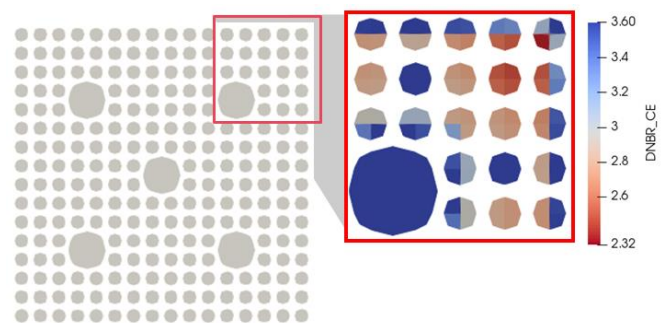


Fig. 8. DNBR distribution with mixing vane model

3.2. Assembly with center-maximum power density (assembly 24)

Without mixing vane model, the maximum coolant and cladding surface temperature at the outlet were 599.025 K and 599.629 K at the corner. After the implementation of mixing vane model, the maximum temperatures were reduced to 598.692 K and 599.256 K. The temperature distribution of coolant and cladding were illustrated on Fig. 9 and Fig. 10.

The lateral location of minimum DNBR and axial location of minimum DNBR were not changed. The minimum DNBR is decreased by 0.112 % with mixing vane model. The estimated DNBR distribution is presented on Fig. 11. When the mixing vane model was applied on simulation, the minimum DNBR was slightly reduced. Since coolant temperature is maximized on the corner subchannel while maximum power density is on the center subchannel, the effect of mixing vane model is relatively diminished.

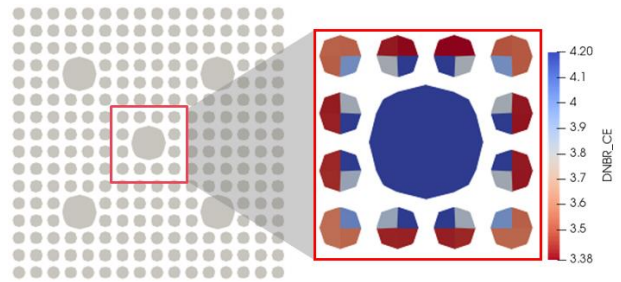


Fig. 11. DNBR distribution with mixing vane model

4. Conclusion

In this paper, the mixing vane model and DNBR calculation model were implemented for subchannel scale T/H analysis. The mixing vane model used for CTF was modified to consider the difference between the collocated and staggered grid systems. The adjusted model was implemented on mass, momentum and energy equation of CUPID. Furthermore, CE-1 CHF correlation was added to capture the effect of mixing vane model on DNBR distribution.

Thereafter, the preliminary simulation for single assembly of APR1400 was progressed. The coolant and cladding surface temperature distribution and DNBR was calculated within two non-uniform power densities. With the mixing vane model, the maximum temperature of coolant and cladding surface were decreased. On the other hand, the effect of mixing vane on DNBR was depended on shape of power ratio.

In the future, validation of model against experiment result will be produced and considering of lateral convection coefficient is needed to be progressed.

ACKNOWLEDGEMENT

This work was supported by National R&D program through the Ministry of Education of the Republic of Korea and National Research Foundation of Korea (NRF). (No. NRF-2017M2A8A4018490)

REFERENCES

- [1] R. Salko, M. Avramova, CTF Theory Manual, Pennsylvania State University, 2014.
- [2] Korea Atomic Energy Research Institute, "CUPID Code Manuals Vol. 1: Mathematical Models and Solution Methods Version 1.9", 2014.
- [3] L. S. Tong, Y. S. Tang Boiling heat transfer and two-phase flow, CRC press, 1997.
- [4] Y. S. Jung, C. B. Shim, C. H. Lim, H. G. Joo, Practical numerical employing direct whole core neutron transport and subchannel thermal/hydraulic solvers, Annals of Nuclear Energy, Vol. 62, pp. 357-374, 2013.
- [5] T. S. Blyth, M. Avramova, Development and Implementation of CFD-Informed Models for the Advanced Subchannel Code CTF, Consortium for Advanced Simulation of LWRs (CASL), 2017.
- [6] A. RUBIN et al., OECD/NRC Benchmark based on NUPEC PWR subchannel and bundle tests (PSBT), Volume I: Experimental Database and Final Problem Specifications. US NRC OECD Nuclear Energy Agency, 2010.

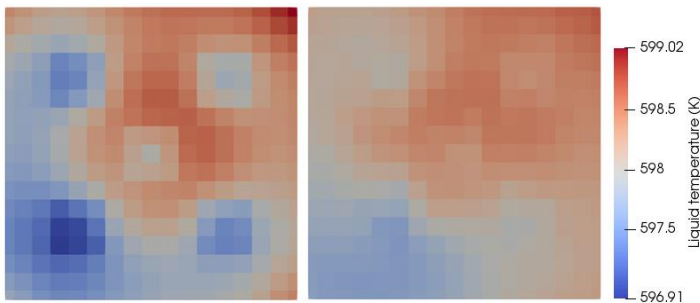


Fig. 9. Outlet coolant temperature distribution without mixing vane model (left) and with mixing vane model (right)

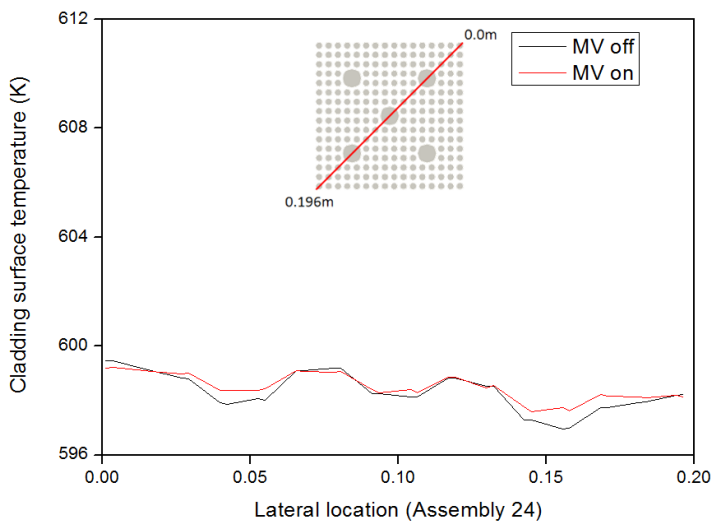


Fig. 10. Outlet cladding surface temperature distribution using power density of assembly 24